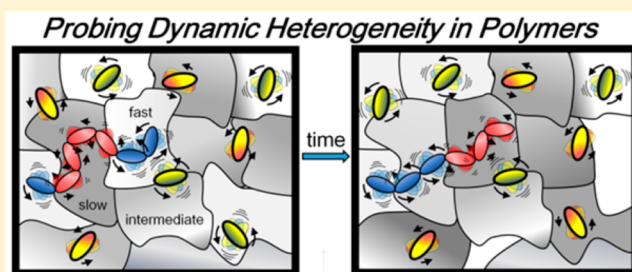


Single Molecule Experiments Reveal the Dynamic Heterogeneity and Exchange Time Scales of Polystyrene near the Glass Transition

Keewook Paeng^{†,‡} and Laura J. Kaufman^{*,†}[†]Department of Chemistry, Columbia University, New York, New York 10027, United States[‡]Department of Chemistry, Sungkyunkwan University, Suwon 440-746, Republic of Korea

ABSTRACT: In a polymeric material near its glass transition temperature, segmental dynamics of a given spatial region may differ considerably from that of neighboring regions without apparent structural origin, analogous to the supercooled liquid state of low molecular weight glass formers. Given that the supercooled liquid state is a (metastable) equilibrium state, spatial variations in dynamics are expected to average out in time, consistent with ergodicity of the system. By probing the rotations of fluorescent guest molecules, local segmental dynamics of polystyrene was scrutinized molecule by molecule. Two perylene dicarboximide dyes were investigated as potential reporters, and one of these was found to report a substantial proportion of the dynamic heterogeneity of the host polystyrene. Using this probe, we demonstrate that the polystyrene system is ergodic and characterize time scales over which molecules experience changes to their dynamics. We identify a characteristic time scale of exchange much longer than the structural relaxation of the host segmental dynamics, consistent with both previous studies on polystyrene and studies on small molecule glass formers. Moreover, we show that dynamic exchange spans a wide range of time scales from <150 to ~35 000 times the segmental relaxation time of the polystyrene.



I. INTRODUCTION

The properties of glass-forming systems remain of great interest for reasons both fundamental and applied. Applied questions are particularly relevant in polymers, which are used in a wide range of technological applications. Fundamentally, these systems are intriguing due to their unusual properties that are intimately related to the glass transition, a phenomenon that remains the focus of significant continued theoretical attention.¹

Among the properties of supercooled liquids and polymeric melts that have piqued the most interest is the apparent broad array of relaxation times in these systems observed in frequency and time-dependent measurements. In the time domain, the presence of this distribution of relaxation times manifests as correlation functions that exhibit the Kohlrausch–Williams–Watts, or stretched exponential, form, $C(t) = C(0) \exp[-(t/\tau_{fit})^\beta]$, with $\beta < 1$. This deviation from exponential behavior has been interpreted as an indicator of dynamic heterogeneity, the presence of sets of molecules with distinct relaxation time scales distributed in space and time across the system.^{2–4} To clarify the spatial extent and temporal persistence of these relaxations with distinct time scales, a variety of subensemble and single molecule experiments have been employed. In polymeric systems, much attention has recently focused on thin polymeric films both above and below the bulk glass transition temperature.^{5,6} Earlier work on amorphous polymers characterized bulk properties such as relaxation time as a function of

temperature, often as a function of either monomer identity or polymer molecular weight.⁷

In polymeric systems near the glass transition, most single molecule work to date has monitored changes in fluorescence lifetime (FL) of probe molecules embedded in a host polymer, as FL fluctuations occur due to changes in position or polarizability of the probe or surrounding host.⁸ Other single molecule studies have assessed the rotation of probe molecules in polymeric systems through measurements of probe linear dichroism, the most common single molecule approach to studying small molecule supercooled liquids.⁹ A few recent studies have monitored translational dynamics of probe molecules in polymers, which requires subdiffraction limit localization, to reveal local translational dynamics within a glassy polymer.^{10–12} While these studies have helped uncover some characteristics of dynamic heterogeneity in bulk amorphous polymers, limitations relating to probe size and subsequent probe averaging in space and/or time over potential heterogeneities in the polymeric systems have complicated analysis.⁹ In this study, we demonstrate that a compact perylene dicarboximide probe mirrors both the segmental dynamics and heterogeneity of those dynamics in polystyrene in the supercooled regime while a larger perylene dicarboximide probe does not. Analyzing probe characteristic relaxations as a

Received: January 14, 2016

Revised: March 9, 2016

Published: March 23, 2016

function of experimental trajectory length allows identification of the time scales over which distinct environments randomize. The range of time scales over which this dynamic exchange occurs in a supercooled polystyrene melt is considered in the context of similar experiments in the small molecule supercooled liquid *o*-terphenyl and previous subensemble experiments in polystyrene.

II. MATERIALS AND METHODS

Sample Preparation. Polystyrene (Polymer Source) with $M_w = 168$ kg/mol, PDI = 1.05 was dissolved in toluene and precipitated in hexane three times. The toluene solution of 3.1 wt % polystyrene was photobleached in a home-built, high power light emitting diode (LED) based photobleaching setup for at least 48 h to achieve a fluorescence-free host matrix. The substrate, a silicon wafer, was cut into $\approx 6.5 \times 6.5$ mm pieces and cleaned with piranha solution ($\text{H}_2\text{SO}_4:\text{H}_2\text{O}_2 = 3:1$). Two fluorescent probes were employed in this experiment: N,N' -bis(2,5-di-*tert*-butylphenyl)-3,4,9,10-perylene-dicarboximide (tbPDI) and N,N' -dipentyl-3,4,9,10-perylene-dicarboximide (pPDI), each obtained from Sigma-Aldrich. In both cases, fluorescent probe solution was mixed with polystyrene solution (1:100 dilution of fluorescent probe solution (5×10^{-9} M) to polymer solution) and spin-coated (2000 rpm) onto a cleaned silicon wafer. Film thickness was ≈ 200 nm as measured by ellipsometry (J.A. Woollam, alpha-SE).

Imaging. Single molecule rotation was studied using a home-built microscope in a wide-field configuration equipped with a vacuum cryostat (Janis, ST-500) for temperature control. Measurements were performed under vacuum, with typical pressure ≈ 1.0 mTorr. Upon placing a sample in the cryostat, the temperature was raised above the glass transition temperature ($T_g \approx 375$ K¹³) and held there for at least 2 h. This procedure (1) stabilizes the vacuum pressure, which limits defocusing during measurements, (2) promotes residual solvent evaporation from the sample, and (3) allows film relaxation, which is important when the measurement temperature is at or below the calorimetric T_g .

Following equilibration as described above, fluorescence from individual probe molecules was collected. Specifically, light from a continuous wave diode laser (Nd:Vanadate 532 nm) was coupled into a multimode fiber, and the fiber was shaken by a home-built shaker that utilizes a speaker to physically shake the fiber at a constant frequency and amplitude to create a randomly polarized, homogeneously illuminated field of view. The laser light was focused at the back of the objective lens (Zeiss, LD Plan-Neofluar, air 63 \times , NA = 0.75, WD = 1.5 mm), resulting in a field of view of ≈ 100 μm diameter. The fluorescence was collected by the same objective lens and passed through a dichroic mirror followed by long-pass and band-pass filters. A Wollaston prism split the image into two orthogonal polarizations that were imaged onto an electron multiplying charge-coupled device camera (EMCCD; Andor iXon DV887).

Excitation power varied from 5–15 mW at the back of the objective lens, corresponding to power density of 50–150 W/cm² at the sample. Frame rate was chosen to be ≈ 20 frames per median relaxation time. Movies with frame rate >5 Hz were collected continuously while slower frame rate movies were collected with 0.2 s exposure time, with illumination shuttered between frames to limit photobleaching. For each data set, several movies at each temperature were collected, and typically >1000 single molecules were analyzed at each temperature for each data set (Tables 1–3). Because of the relatively high power density excitation used in single molecule measurements, sample heating relative to the set temperature can occur. Actual temperature of samples used in this report was estimated using power dependence measurements of tbPDI in *o*-terphenyl.¹⁴ Excitation power dependence of the rotational correlation time in that system was measured for shuttered and continuous movies and found to be -0.00124 decades/mW and -0.00995 decades/mW. The changes in rotational correlation time were converted to temperature changes using the temperature dependence of the dielectric relaxation time of *o*-terphenyl,¹⁵ which resulted in 0.0048 and 0.0418 K/mW for shuttered and continuous movies, respectively. Because the host matrices do not

absorb at the excitation wavelength, sample heating is expected to result from substrate heating; thus, the temperature increase as a function of excitation power is expected to be host independent and values obtained from *o*-terphenyl were applied in the current polystyrene system.

Data Analysis. From the two orthogonal polarization images collected on the CCD at each time point, polarized fluorescence intensities of each single molecule (I_s, I_p) were extracted, and single molecule linear dichroism (LD) was calculated via $\text{LD}(t) = (I_s - I_p) / (I_s + I_p)$. An autocorrelation of $\text{LD}(t)$ was constructed via $[\sum_{i=1}^n a(t') \times a(t' + t)] / [\sum_{i=1}^n a(t') \times a(t')]$ where $a(t) = \text{LD}(t) - \langle \text{LD}(t) \rangle$. Data analysis from image processing through autocorrelation construction was performed as described in ref 16.

Each autocorrelation function was then fit to a stretched exponential function ($C(t) = C(0) \exp[-(t/\tau_{\text{fit}})^\beta]$) with least-squares fitting until the correlation function decayed to 0.1. β and $C(0)$ values were constrained to $0.2 < \beta < 2.0$ and $0.3 < C(0) < 2.0$. The average rotational correlation time, τ_c , was calculated from the fit values of τ_{fit} and β via $\tau_c = (\tau_{\text{fit}}/\beta) \cdot \Gamma(1/\beta)$, where Γ is the gamma function. Molecules with (number of frames)/ $\tau_{\text{fit}} \leq 2$ and trajectory length $\leq 10 \tau_{\text{fit}}$ were excluded from further analysis. All data analysis was performed using IDL software (ITT Visual Information Solutions).

III. RESULTS

Temperature Dependence. The autocorrelation of linear dichroism as measured in the experimental configuration used in this study has been shown to be strongly dominated by the second rank orientational correlation function,^{17,18} reflecting the rotational relaxation of the probe molecules. To ensure probe rotations reflect the dynamics of the host polystyrene matrix, probe temperature dependence was investigated and compared to the temperature dependence of bulk polystyrene measured previously. For both tbPDI and pPDI probes, linear dichroism autocorrelation functions of more than 1000 molecules at each analyzed temperature were constructed and fit to stretched exponential decays as described in [Materials and Methods](#). Resulting mean rotational correlation time, τ_c , was

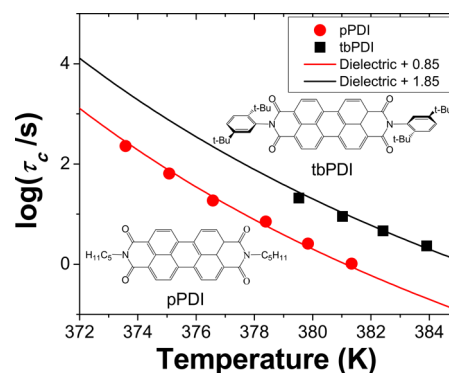


Figure 1. Temperature-corrected τ_c measurements of pPDI (red) and tbPDI (black) in polystyrene at temperatures near T_g . The lines drawn are the Vogel–Fulcher–Tammann fits to the temperature dependence of polystyrene as measured by dielectric spectroscopy by Roland and co-workers.²² The dielectric line is shifted by 0.85 and 1.85 decades to match the pPDI and tbPDI rotational correlation times, respectively. Chemical structures of the two probe molecules are also shown.

plot as a function of temperature. A variety of experiments previously measured the temperature dependence of bulk polystyrene segmental relaxation, primarily via dielectric spectroscopy.^{19–23} Among these data sets, slight variations exist, particularly at the lowest temperatures measured. In this study, the temperature dependence of relaxation times

Table 1. Temperature Dependence of pPDI in Polystyrene ($494\tau_{fit,med}$ Trajectory Set)

	373.6 K	375.1 K	376.6 K	378.4 K	379.8 K	381.3 K	combined
number of molecules	1080	1113	1310	1289	1356	1424	7572
median τ_c (s)	228.15	64.61	18.73	7.08	2.57	0.54	1
median τ_{fit} (s)	118.86	32.63	9.55	3.61	1.31	1.03	1
median β	0.55	0.54	0.54	0.54	0.53	0.56	0.54
median trajectory ($\tau_{fit,med}$)	429	536	559	554	512	463	494
median frame rate (frames/ τ_{fit})	22.0	18.1	17.4	18.0	19.5	21.6	19.3
fwhm (τ_c distribution)	0.58	0.52	0.50	0.49	0.50	0.56	0.52
fwhm (τ_{fit} distribution)	0.57	0.53	0.50	0.50	0.52	0.50	0.51
fwhm (β distribution)	0.40	0.37	0.36	0.37	0.34	0.36	0.37
β_{QE}	0.53	0.52	0.52	0.52	0.52	0.53	0.52

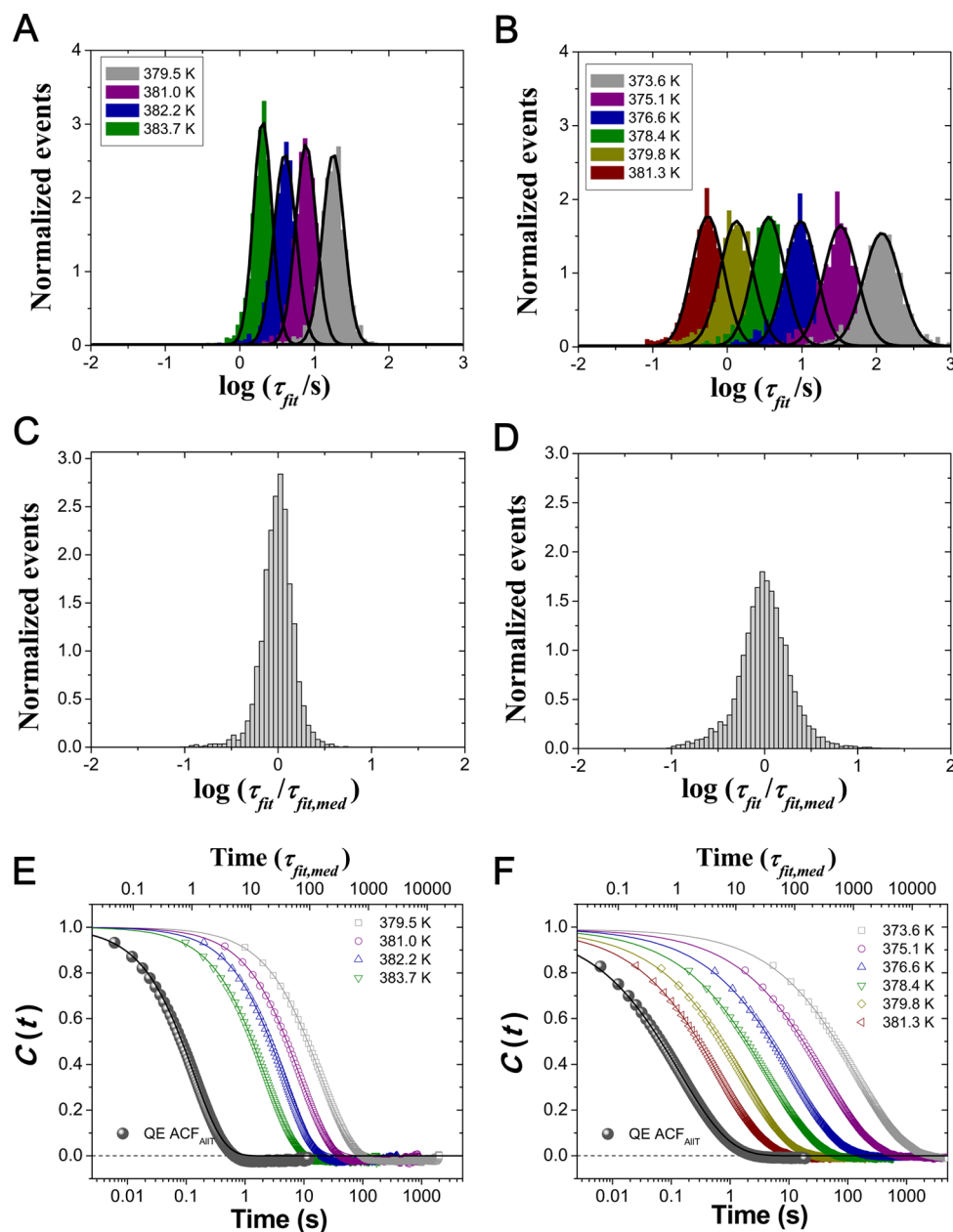


Figure 2. Details of tbPDI (left) and pPDI (right) rotational relaxation in polystyrene: (a, b) τ_{fit} distributions for each temperature interrogated, (c, d) temperature-combined τ_{fit} histograms: fwhm for tbPDI is 0.33 and for pPDI is 0.51, and (e, f) quasi-ensemble ACFs (ACF_{QE}s) from each measured temperature as well as from temperature-combined data. Stretched exponential decays for the temperature-combined data yield $\beta_{QE} = 0.84$ for tbPDI and $\beta_{QE} = 0.52$ for pPDI. The histograms (a–d) are normalized by the area under the curve.

measured with both pPDI and tbPDI probes matches best with the dielectric measurements of Roland et al.²²

Figure 1 shows the measured temperature dependence of the rotational correlation times of pPDI and tbPDI in bulk polystyrene. Because tbPDI rotates more slowly than pPDI at a given temperature, the lowest temperatures probed are only explored with pPDI. Figure 1 reveals that the rotational relaxation dynamics of pPDI and tbPDI molecules track the temperature dependence of the segmental relaxation of polystyrene as assessed through a probe-free dielectric study.²² Dielectric spectroscopy data for 90 kg/mol PS from ref 22 was taken and fit to the Vogel–Fulcher–Tammann (VFT) description of the temperature dependence ($\log(\tau/\tau_0) = B/(T - T_0)$) with τ_0 , B , and T_0 constants), with T_0 fixed to 341.3 K as in the original work, yielding $\log(\tau_0) = -11.25$ and $B = 414.15$ K. This line fits well to our measured τ_c data when shifted to reflect the slower relaxations of the probe molecules (0.85 decades for pPDI and 1.85 decades for tbPDI) relative to the inherent polystyrene segmental relaxation. This consistency with previously measured temperature dependence of bulk polystyrene assures the probe is slaved to the dynamics of the host. It also assures the polystyrene film is sufficiently thick to not show thin film effects, as these would be expected to be more dominant at lower temperatures, resulting in deviations from known bulk polystyrene temperature dependence near T_g .^{19,20}

Relaxation Rate Distributions. While Figure 1 demonstrates that tbPDI and pPDI both follow the known temperature dependence of polystyrene segmental dynamics, these probes may or may not report all dynamic heterogeneity in the system. We further explore the details of polystyrene dynamics reported by tbPDI and pPDI through assessing the distributions of relaxation times for at least 1000 of each of the two types of probe molecules at each temperature probed (Tables 1 and 2, Figure 2). In Figure 2, τ_{fit} distributions are plot for each temperature measured for both probes. While τ_c captures average rotational relaxation time, τ_{fit} captures the decay of the first portion of the linear dichroism autocorrelation function, providing a measure of how fast the majority of the rotational relaxation occurs.

For both pPDI and tbPDI, the τ_{fit} distributions are broad, largely log-normal, and display no apparent change in shape as a function of temperature in the range probed. Given this temperature invariance, data collected at all temperatures is combined into a single histogram normalized by median relaxation time at each temperature (Figure 2c,d). The width of such relaxation time distributions has previously been used to assess host heterogeneity as reported by single molecule probes, since probes experiencing a dynamically homogeneous environment would be expected to return a very narrow distribution of time scales. For tbPDI in polystyrene, the fwhm of the temperature combined $\log(\tau_{\text{fit}})$ distribution is found to be 0.33 while that of the pPDI data is 0.51. Because tbPDI is less photostable in polystyrene than is pPDI, the obtained trajectories are significantly shorter for tbPDI (116 τ_{fit} in length) than for pPDI (494 τ_{fit}). Short trajectories can contribute to wide distributions of τ_{fit} and τ_c through two mechanisms. First, short trajectories can broaden distributions for statistical reasons; second, short trajectories may lead to wide relaxation time distributions if there is significant heterogeneity in the system but dynamic exchange between environments occurs on time scales longer than those accessed in the experiment.^{14,24–27} Despite this tendency for relaxation

Table 2. Temperature Dependence of tbPDI in Polystyrene (116 $\tau_{\text{fit,med}}$ Trajectory Set)

	379.5 K	381 K	382.4 K	383.9 K	combined
number of molecules	1187	1305	1836	1377	5705
median τ_c (s)	20.97	8.99	4.65	2.31	1
median τ_{fit} (s)	17.86	7.64	4.02	2.01	1
median β	0.83	0.85	0.86	0.85	0.85
median trajectory ($\tau_{\text{fit,med}}$)	116	122	105	127	116
median frame rate (frames/ τ_{fit})	17.9	17.0	20.1	20.7	19.0
fwhm (τ_c distribution)	0.37	0.37	0.37	0.31	0.35
fwhm (τ_{fit} distribution)	0.34	0.33	0.35	0.29	0.33
fwhm (β distribution)	0.55	0.54	0.58	0.55	0.56
β_{QE}	0.80	0.82	0.84	0.84	0.84

time distributions to be broader for data of short trajectory length, the tbPDI distributions are significantly narrower than those of pPDI despite tbPDI trajectories being much shorter than pPDI trajectories. Indeed, constructing pPDI trajectories of equal length to those collected for tbPDI by creating autocorrelations from only the early portion of longer collected trajectories yielded $\log(\tau_{\text{fit}})$ distributions with a fwhm of 0.73 for pPDI compared to that of 0.33 for tbPDI trajectories of the same length. Taken together, these results suggest that the narrow distribution of tbPDI relaxation times measured in PS reflects an inability for that probe to report the full heterogeneity in the system.

The possibility that tbPDI has limited capacity to report dynamic heterogeneity in polystyrene compared to pPDI can be further investigated by examining quasi-ensemble autocorrelation functions (ACF_{QE}). These are constructed by adding the full set of single molecule autocorrelations collected at each temperature; each ACF_{QE} is then fit with best-fit stretched exponential functions, yielding $\tau_{\text{fit,QE}}$, β_{QE} , and $\tau_{c,\text{QE}}$. The ACF_{QE} functions (as well as a temperature-combined ACF_{QE} for pPDI and tbPDI) are shown in Figure 2,e and f. Unlike the width of the distribution of relaxation times, ACF_{QE} functions are rather insensitive to trajectory length, as they do not vary with limited dynamic exchange so long as sufficient molecules are included.^{26,28} For tbPDI, β_{QE} at each measured temperature is ~ 0.84 while those constructed from pPDI trajectories yield $\beta_{\text{QE}} = 0.52$. This confirms that pPDI is reporting more heterogeneity in polystyrene than is tbPDI. Moreover, the stretching exponent obtained from pPDI is similar to those obtained from both probe-free and small probe-bearing ensemble measurements in polystyrene.^{22,29–31} From these results and other observations on probe ability to report heterogeneity in supercooled liquids,^{28,32–34} we conclude that tbPDI rotates too slowly to report the full breadth of dynamic heterogeneity of the segmental dynamics of polystyrene while pPDI is sufficiently small and fast to report the great majority of that heterogeneity. We note that pPDI rotates ~ 0.85 decades slower ($\sim 7\times$) while tbPDI rotates 1.85 decades slower ($\sim 70\times$) than polystyrene's segmental or α -relaxation time (τ_α) as reported by dielectric measurements. This suggests that significant dynamic exchange occurs between the two minimum time scales these probes can report, consistent with conclusions drawn from probe dependent measurements in small molecule and polymeric glass formers.³⁴ While tbPDI may not report the full breadth of heterogeneity in polystyrene segmental dynamics, the non-unity β_{QE} reported by tbPDI in polystyrene

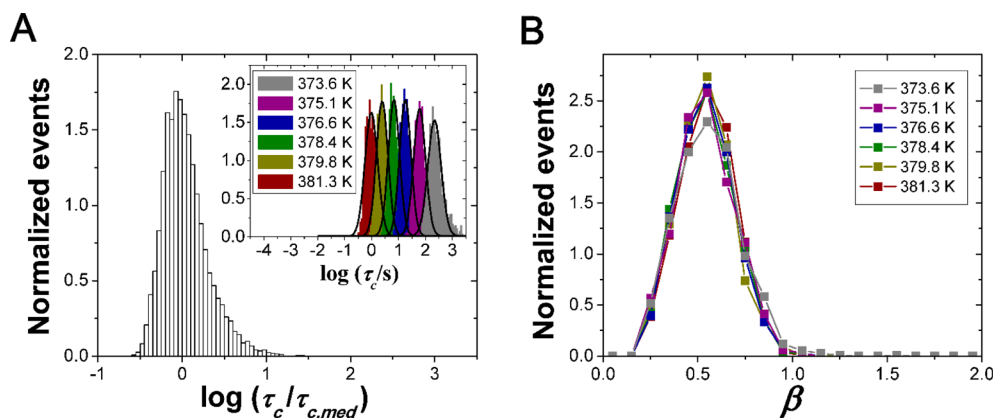


Figure 3. Additional parameters obtained from pPDI measurements in polystyrene. (a) Temperature-combined τ_c histogram with (inset) τ_c distributions for each temperature interrogated. Black lines are best-fit Gaussian fits. (b) β distribution for each measured temperature. Lines are guides to the eye.

suggests that some exchange also occurs on time scales beyond those averaged over during tbPDI rotations.

Given the result that pPDI reports a more substantial portion of dynamic heterogeneity in polystyrene than tbPDI, we assess results from pPDI rotations in polystyrene in more detail. While the stretching exponents obtained from the ACF_{QE} s provide a measure of total heterogeneity in the system, analyzing the full distribution of relaxation times reported by individual molecules and how these change with time of monitoring provides information on how this heterogeneity is apportioned in space and time. Thus, for each molecule we plot not only τ_{fit} (Figure 2) but also τ_c and β (Figure 3). As for τ_{fit} distributions, τ_c distributions are found to be shape invariant as a function of temperature, and thus we combine data from all temperatures into a single histogram (Figure 3a). From this histogram, it is apparent that while τ_{fit} is nearly log-normal, τ_c demonstrates additional intensity in the long time tail relative to a log-normal. The β distributions also do not vary with temperature: all demonstrate nearly normal distributions with a fwhm of ~ 0.37 and average median $\beta = 0.54$ (Figure 3b, Table 1). We note that the median β value is similar to the β_{QE} value of 0.52, indicating that many pPDI molecules have experienced most dynamic environments in the host by the end of the ~ 500 τ_{fit} trajectories.

As described in recent work investigating a small BODIPY probe in the small molecule glass former *o*-terphenyl,¹⁴ if a single molecule probe reports heterogeneity in a host, the full set of dynamic environments, τ , that the molecule experiences can be extracted through an inverse Laplace transform (ILT),

$$\exp[-(t/\tau_{fit})^\beta] = \int_{-\infty}^{\infty} P(\log \tau; \tau_{fit}, \beta) \exp(-t/\tau) d[\log \tau]$$

Doing so for every pPDI single molecule trace and summing these distributions as described in ref 14 results in the set of relaxation times shown in Figure 4 and represents the full breadth of dynamic environments experienced and reported by the pPDI probes. We term this distribution the ILT-built distribution, and it matches well with the ILT of the quasi-ensemble data (Figure 4, red line), thus validating the ILT-built distribution as returning the full set of dynamic environments reported.

Trajectory Length Dependence. In the pPDI in polystyrene data presented above, median β values are quite similar to β_{QE} values (Figure 2f, 3b, and Table 1). This indicates

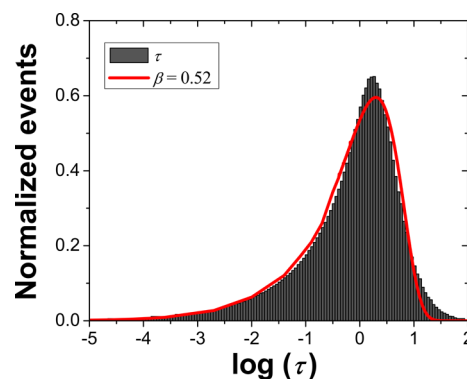


Figure 4. ILT-built distribution composed of the ILT of each single molecule autocorrelation (histogram) and the ILT of a stretched exponential with $\beta = 0.52$ (red line), the β value obtained from the temperature-combined ACF_{QE} of pPDI in polystyrene.

that many pPDI molecules have experienced most of the temporal environments present in the polystyrene by the end of the experiment. However, if all molecules experienced and reported all accessible dynamic environments, a very narrow distribution of β values (fwhm < 0.2) would be expected, broadened only from a delta function due to statistical fluctuations associated with finite trajectory length.²⁶

To determine both the time required for a *typical* molecule to access all dynamic environments present and the time required for *all* molecules to access those environments, we examine the behavior of pPDI τ_{fit} , β , and τ_c distributions as a function of trajectory length (Figure 5). The pPDI probes were found to be very photostable in polystyrene relative to probe/host pairs investigated previously; as such, extremely long trajectory lengths were obtained when low power excitation was used. Figure 5 shows τ_{fit} , β , and τ_c distributions for trajectories from ~ 500 to more than 2000 τ_{fit} (Table 3). In addition, shorter trajectories were crafted from analyzing portions of longer trajectories: trajectories of 273, 109, 54, and 27 τ_{fit} were obtained from 924 τ_{fit} trajectories. In all cases, except for the 494 τ_{fit} trajectories measured at 6 temperatures, this data was collected at the single temperature of 378.4 K. Figure 5 reveals that as trajectory length increases, the measured τ_{fit} and τ_c distributions become narrower. This is consistent with the expectation for an ergodic system, where at infinite trajectory length a delta function would be expected for

Table 3. Trajectory Length Dependence of pPDI Probe in Polystyrene

	$2369\tau_{\text{fit,med}}$	$1424\tau_{\text{fit,med}}$	$940\tau_{\text{fit,med}}$	$494\tau_{\text{fit,med}}$	$273\tau_{\text{fit,med}}$	$109\tau_{\text{fit,med}}$	$54\tau_{\text{fit,med}}$	$27\tau_{\text{fit,med}}$
number of molecules	1160	801	1311	7572	1937	2126	1894	1563
median τ_c	9.23	7.87	7.40	1	6.19	5.11	3.91	2.82
median τ_{fit}	4.46	3.85	3.66	1	3.46	3.30	2.83	2.27
median β	0.50	0.51	0.52	0.54	0.59	0.66	0.78	0.89
median frame rate (frames/ τ_{fit})	22.3	19.3	18.3	19.3	17.3	16.5	14.2	11.3
fwhm (τ_c distribution)	0.31	0.37	0.44	0.52	0.58	0.72	0.83	0.83
fwhm (τ_{fit} distribution)	0.28	0.36	0.43	0.51	0.61	0.73	0.85	0.86
fwhm (β distribution)	0.19	0.24	0.30	0.37	0.45	0.60	0.77	1.08
β_{QE}	0.50	0.50	0.51	0.52	0.53	0.58	0.62	0.72
ILT-built mismatch (%)	1.77	2.99	4.22	5.94	8.67	13.33	25.61	42.61

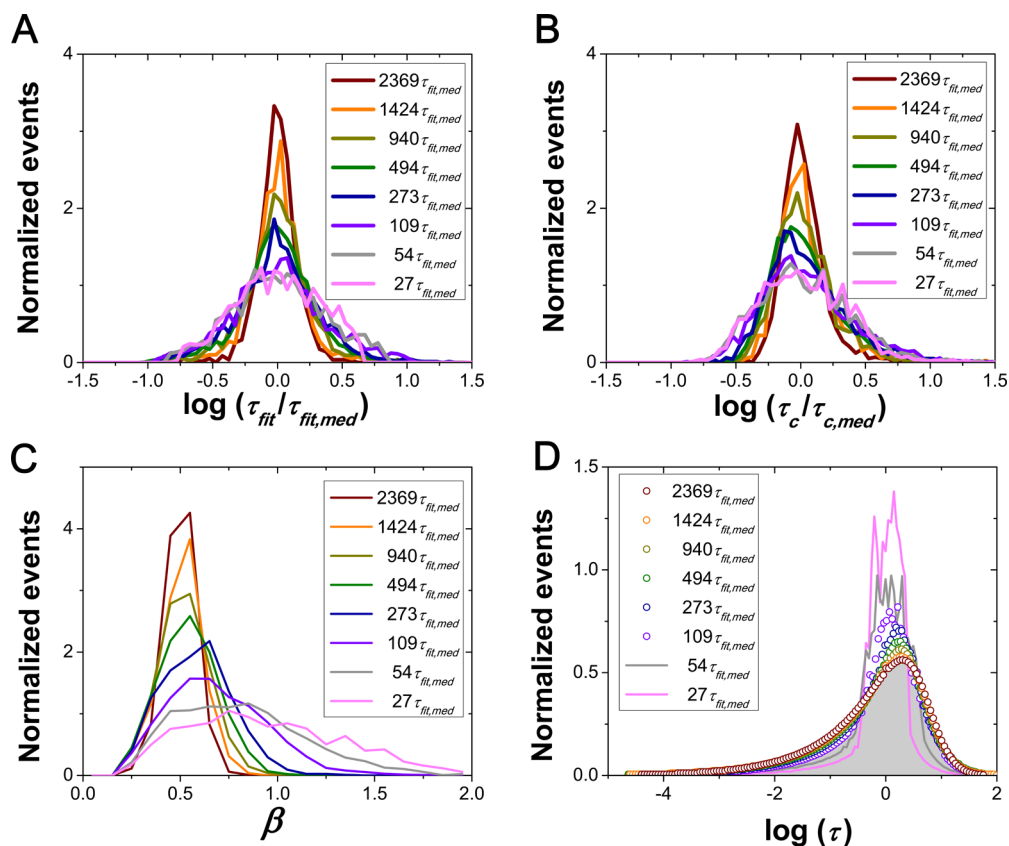


Figure 5. Rotational relaxation parameters for pPDI probes in polystyrene as a function of trajectory length. Details associated with each measurement are provided in Table 3 and the text. (a) Normalized τ_{fit} distributions, (b) normalized τ_c distributions, (c) β distributions, and (d) ILT-built distributions associated with autocorrelation functions from each data set.

each of these distributions. Similarly, the β distribution becomes narrower as trajectory length increases. The β distribution also shifts to the left, evolving from a median near one to a median of $\beta = 0.50$, equivalent to the β_{QE} value, by trajectory lengths of $\sim 1000 \tau_{\text{fit}}$.

While the distributions of τ_{fit} , β , and τ_c are expected to evolve with trajectory length, the ILT-built distribution is not, as this reflects the full distribution of time scales explored, regardless of whether this emerges from many molecules exploring single dynamic environments or one or more molecules each exploring all the environments present in the system. For trajectories of $109 \tau_{\text{fit}} - 2369 \tau_{\text{fit}}$ in length, very stable ILT-built distributions are found. For the two shortest trajectories, the ILT-built distributions are narrower than those constructed from longer trajectories. This effect is likely related to the limited dynamic range of the experiment as it was performed in

this study. For the shortest trajectories collected, most molecules are expected to experience a single dynamic environment within the range of time scales associated with the ILT of a stretched exponential with $\beta = 0.52$. As can be seen in Figure 4, this spans approximately 5 decades. However, data was collected at a single frame rate chosen to best match the rotational dynamics of the average molecule, a frame rate that cannot capture relaxations more than approximately a decade faster or slower than the time scale for which it was chosen. As a result, the distribution of time scales obtained from the short trajectory data does not represent all of the time scales present, and the ILT-built distribution does not match that obtained from longer trajectory length data.

To further quantify the exchange time distribution that exists in bulk polystyrene, we note that within each data set, there are molecules with both shorter and longer trajectories than the

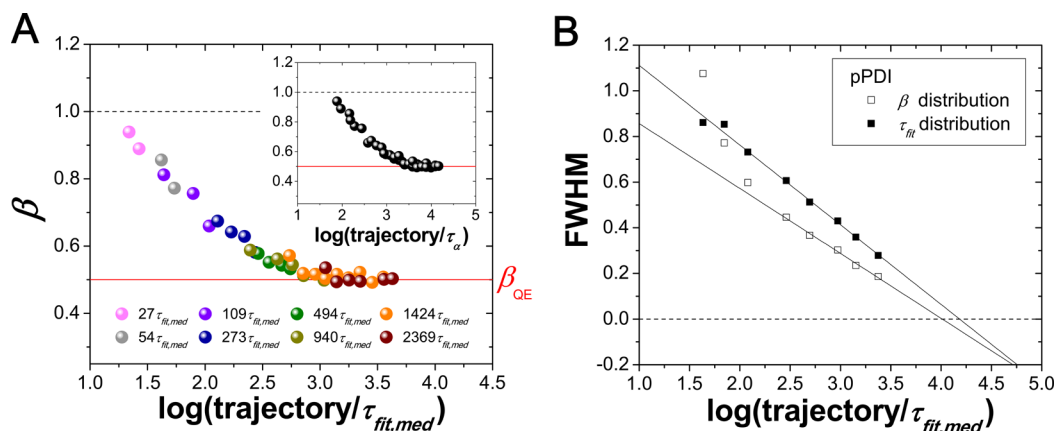


Figure 6. (a) Median β for pPDI in polystyrene as a function of trajectory length in terms of τ_{fit} for subsets of data within given data sets of particular median trajectory length. Inset shows the same data as a function of trajectory length in terms of τ_{α} . (b) fwhm of τ_{fit} (in units of $\log(\tau_{\text{fit}}/\tau_{\text{fit,med}})$) and β (unitless) distributions as a function of trajectory length in terms of τ_{fit} . Lines are best linear fits to the data, with the three shortest trajectory data points excluded for the β distribution data, consistent with fwhm of β values being strongly dominated by statistics at short trajectory lengths.^{25,26}

median value given in Table 3. Analyzing median β value of subsets of trajectories as a function of trajectory length within and across data sets provides a more detailed view of the evolution of β with trajectory length. Figure 6a shows how the median β value evolves with trajectory length for pPDI in polystyrene. Deviation of β below 1 is already seen for trajectories of $\sim 30 \tau_{\text{fit}}$ length, where $\beta \sim 0.90$. Such trajectories can also be expressed in terms of rotational correlation time, τ_c and these trajectories are $\sim 22 \tau_c$ in length (Table 3). Because pPDI's rotational correlation time is ~ 7 times slower than the segmental relaxation time of polystyrene, this implies that by ~ 150 times the segmental relaxation time of polystyrene, exchanges are occurring. This is consistent with tbPDI reporting a higher β value at identical trajectory length than pPDI in polystyrene, as tbPDI cannot report on exchanges that occur faster than ~ 700 times τ_{α} given that $\tau_c/\tau_{\alpha} = 70$ for this probe/host pair and we consider trajectories of $\sim 10 \tau_c$ the shortest than may return a meaningful β value. For pPDI, the further decay of median β value to ~ 0.50 occurs smoothly until it plateaus at a trajectory length of $\sim 630 \tau_{\text{fit}}$. This indicates that a typical molecule has experienced the great majority of the dynamical environments in the system by approximately 2,300 times the average segmental relaxation time of polystyrene at all temperatures in the supercooled regime explored here. To estimate the time scale on which all pPDI molecules have experienced the full set of dynamic environments in the system, we examine the breadth of the τ_{fit} and β distributions, which approach zero as all molecules experience all environments. Figure 6b suggests that all molecules experience the full breadth of dynamic environments in the system by $\sim 10\,000 \tau_{\text{fit}}$ or $\sim 35\,000$ times the average segmental relaxation time. Taking the data together, evidence of dynamic exchange in the segmental dynamics in bulk polystyrene exists from <150 to $35\,000 \tau_{\alpha}$ and the typical molecule experiences all environments in the system by $\sim 2300 \tau_{\alpha}$.

IV. DISCUSSION

Single molecule measurements of the rotations of PDI dyes in bulk polystyrene reveal that tbPDI probes only report a subset of the dynamic environments present in polystyrene while pPDI probes report a much greater proportion of those environments, returning stretching exponents similar to those obtained from probe-free studies. For pPDI in polystyrene, τ_{fit}

distributions are found to be nearly log-normal while the distributions of rotational relaxation time, τ_c have a long-time tail, even on a log plot. No trend in distribution shape as a function of temperature is seen in either τ_{fit} or τ_c in the temperature regime studied here for either probe ($1.00\text{--}1.02 T_g$ for pPDI and $1.01\text{--}1.02 T_g$ for tbPDI), though we note that this may be too small a temperature range to reveal any such changes.³⁵ Studying behavior of single molecule relaxations as a function of trajectory length from ~ 25 to greater than 1000 times the average rotational relaxation time of the pPDI probes confirms that these systems are ergodic. First, ILT-built distributions, which are sensitive to spatial and temporal heterogeneity, are generally stable as a function of trajectory length while relaxation time and β distributions evolve, consistent with a shift from domination by spatial to temporal descriptions of dynamic heterogeneity with longer observation. Additionally, it is apparent that significant exchange occurs over the trajectory lengths examined, as median β values decay from ~ 0.90 to 0.50 between ~ 30 and $630 \tau_{\text{fit}}$ before plateauing. After this plateau, relaxation time and β distributions continue to narrow with increasing trajectory length, and extrapolation suggests full ergodicity is restored (all molecules have felt all accessible and reportable dynamic environments in the system) by $\sim 10\,000 \tau_{\text{fit}}$ or $\sim 35\,000 \tau_{\alpha}$.

We note that the trends seen in this study are similar to trends seen in single molecule studies of small molecule glass formers. Notably, probe-dependent studies using PDI probes in both glycerol and *o*-terphenyl revealed that faster rotating probes returned broader relaxation time distributions than slower ones, indicating slow probes average over dynamic exchange in the host.^{28,32} In those studies, however, none of the PDI probes returned median β values that were as close to the ensemble probe-free results as found for the pPDI probes in polystyrene here. This is consistent with the τ_c/τ_{α} value of pPDI in polystyrene being 7 while all PDI probes used in glycerol and OTP had larger ratios.³² While pPDI was not used in any of the previously published work, we have measured the dynamics of pPDI in OTP, which is found to demonstrate $\tau_c/\tau_{\alpha} = 35$, and find that this probe does not return a β value equivalent to probe-free measurements (data not shown). A recent study with BODIPY268 in *o*-terphenyl, with $\tau_c/\tau_{\alpha} = 3$, did return the β value expected from probe-free studies.¹⁴

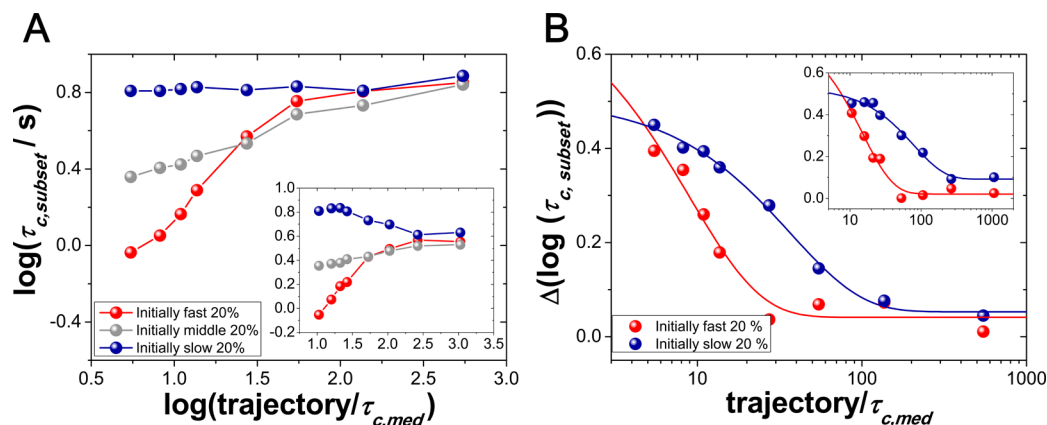


Figure 7. (a) Median τ_c values as a function of trajectory length for three subensembles: the 20% initially fastest (red), initially slowest (blue), and 20% in the middle of the initial τ_c relaxation time distribution. The inset shows the same result expressed as a function of τ_{fit} with the subensembles selected from the initial τ_{fit} relaxation time distribution. (b) Differences in τ_c (or, in inset, τ_{fit}) between the initially 20% fastest or 20% slowest molecules and the middle 20% subensemble of molecules. Solid curves are fits to an exponential decay, yielding fit values of $9 \tau_c$ ($15 \tau_{\text{fit}}$) and $37 \tau_c$ ($79 \tau_{\text{fit}}$) for the fast and slow subensembles, respectively. These τ_c values correspond to characteristic exchange times of $63 \tau_\alpha$ and $259 \tau_\alpha$.

To date, the only single molecule probes that have returned median stretching exponents similar to those expected from probe-free measurements display $\tau_c/\tau_\alpha < 10$ while none with $\tau_c/\tau_\alpha > 10$ have done so.⁹ We note that the quantity τ_c/τ_α does not necessarily scale with molecular weight ratio of the probe and host even for a given host due to intermolecular interactions.²⁸ When comparing between small molecular, network, and polymeric glass formers, one must also consider that the relevant host may not be a single molecule or monomer. For example, pPDI is 2.3 times the molecular weight of *o*-terphenyl while it is more than 5 times the molecular weight of the styrene monomer; however the τ_c/τ_α value is lower in polystyrene, allowing the probe to report the full heterogeneity in this host. Comparing the behavior of the two probe/host systems in which the probe successfully reports the same degree of heterogeneity as probe-free experiments (BODIPY268 in *o*-terphenyl and pPDI in polystyrene), the distribution of exchange times appears to be shifted to somewhat longer times in polystyrene, with the average molecule in OTP recovering ergodicity in $\sim 1000 \tau_\alpha$ and all regions doing so by $\sim 10\,000 \tau_\alpha$ ¹⁴ while those time scales in polystyrene are ~ 2300 and $35\,000 \tau_\alpha$, respectively.

The obtained single molecule results on exchange times present in polystyrene can be compared with those measured previously using tetracene and rubrene in polystyrene.³¹ Here, fluorescence photobleaching was used to monitor the rotational correlation time of an initially slowly rotating subensemble of rubrene probes. The characteristic time required for the subensemble to recover the rotational correlation time of the full ensemble was denoted the exchange time. This study revealed that exchange times were long compared to rotational correlation times of the probe and host molecules and that there was a strong temperature dependence of exchange time, results consistent with similar measurements in *o*-terphenyl.³⁶ While our study does not focus on exchange time as a function of temperature, we find no obvious temperature dependence of exchange time. Our study does find, consistent with the earlier studies, that exchange occurs primarily on time scales significantly longer than the rotational relaxation times of the probe and host. While it is difficult to quantitatively compare the characteristic exchange times obtained in the two studies due to the different probes employed, different molecular

weight of polystyrene used, and different approaches to determining exchange time, our data appears to report longer exchange times than does the earlier study. In that study, characteristic exchange time was found to be in the range of 10–100 times the structural relaxation time of the system, depending on the probe and temperature.³¹ The closest analogue to this characteristic exchange time in the data described here is the time required for the β value as a function of trajectory length to reach β_{QE} , as occurs at $\sim 2300 \tau_\alpha$.

Two key differences between our analysis and the previous analysis are that (1) the analysis presented here considers all molecules while the previous one interrogated a slow subensemble and (2) the analysis presented here considers evolution of β , while the previous analysis considered evolution of τ . To obtain a characteristic exchange time in closer analogy to that described in the earlier study, we performed additional analysis of our data, isolating subsets of fast and slow molecules in the initial distribution and investigating the average time required for those subsets of molecules to recover the median τ_c and τ_{fit} values associated with the full ensemble.

Figure 7 shows the evolution of the dynamics of three subensembles of molecules selected from data collected as a function of trajectory length (data sets presented in Table 3). Here, molecules in data sets of each trajectory length were separated into fifths according to their initial rotational relaxation times. Molecules in the fastest, slowest, and middle fifths of the distribution were chosen for additional analysis. As expected from a system that has recovered ergodicity, all subsets of molecules recover the same median relaxation time for the longest trajectory lengths considered. The time scale on which this recovery takes place can be characterized in analogy to the analysis performed in ref 31. First, subtraction of the median rotational correlation times for data of each trajectory length was performed to compensate for an overall trajectory length dependence of the median rotational correlation time, as can be seen in the increase of rotational correlation time in the middle 20% molecules (Figure 7a, gray line). This overall change occurs in part due to statistical effects associated with short trajectories^{24,25} and in part due to the limited dynamic range of short trajectory experiments. Following this, the evolution of the difference in rotational correlation time between the initially slowest and fastest fifth of molecules

from that of the median as a function of trajectory length was fit to an exponential decay. The time constant obtained from this fit characterizes the time required for the initially slowest and fastest subensembles to recover the rotational correlation time of the average molecule. Doing so yields time scales of $9 \tau_c$ for the fast subensemble and $37 \tau_c$ for the slow subensemble (Figure 7b), corresponding to $63 \tau_\alpha$ and $259 \tau_\alpha$. This analysis shows a small difference in the time scales of recovery of ensemble dynamics between the fast and slow subensembles, with the slow subensemble taking a longer time to return to average dynamics than the fast subensemble. Moreover, this analysis returns characteristic exchange times comparable to those extracted from rubrene in polystyrene in ref 31. This analysis of characteristic exchange time yields shorter time scales than does the analysis of evolution of β , an analysis which showed a typical molecule takes $2300 \tau_\alpha$ to return the stretching exponent associated with the full ensemble. This difference in time scales is expected as, given the ensemble distribution, statistically only a few exchanges will be necessary for a typical molecule to recover the median rotational correlation time while many exchanges will be required for a typical molecule to attain β_{QE} , as attaining that low stretching exponent requires the molecule to explore most dynamic environments in the system. We stress that while different definitions of exchange time are possible, our study clearly reveals that dynamic exchange occurs over a very wide range of time scales including those much longer than the structural or segmental relaxation of the host.

V. CONCLUSIONS

Single molecule linear dichroism measurements of pPDI and tbPDI in polystyrene show that pPDI can report the great majority of dynamic heterogeneity in this host while tbPDI cannot. This is reflected in the β_{QE} values, which for pPDI are nearly as low as those measured previously in probe-free experiments. Further analysis of pPDI data shows that as a function of increasing trajectory length data, distributions of relaxation times narrow and distributions of β values both narrow and shift to lower values while inverse Laplace transform distributions that account for both spatial and temporal heterogeneity are stable as a function of trajectory length; each of these findings is consistent with the idea that non-exponential relaxations found in polymeric systems near the glass transition emerge from sets of distinct dynamic environments that are distributed in space and evolve in time. Time scales over which dynamic exchange takes place were evaluated through scrutiny of evolution of median β and τ_c values as well as their distribution widths as a function of trajectory length. In analogy to previous analysis, a characteristic time scale associated with exchange was identified for a slow subensemble of molecules, yielding $\sim 260 \tau_\alpha$ while the full range of dynamic exchange time scales covers a wide range, with evidence for such exchange from $<150 \tau_\alpha$ to $\sim 35\,000 \tau_\alpha$.

■ AUTHOR INFORMATION

Corresponding Author

*(L.J.K.) E-mail: kaufman@chem.columbia.edu.

Notes

The authors declare no competing financial interest.

■ ACKNOWLEDGMENTS

This work was supported by NSF CHE 1213242. We thank Dat Tien Hoang and Alyssa Manz for helpful discussions.

■ REFERENCES

- (1) Berthier, L.; Biroli, G. Theoretical Perspective on the Glass Transition and Amorphous Materials. *Rev. Mod. Phys.* **2011**, *83*, 587–645.
- (2) Ediger, M. D. Spatially Heterogeneous Dynamics in Supercooled Liquids. *Annu. Rev. Phys. Chem.* **2000**, *51*, 99–128.
- (3) Richert, R. Heterogeneous Dynamics in Liquids: Fluctuations in Space and Time. *J. Phys.: Condens. Matter* **2002**, *14*, R703–R738.
- (4) Richert, R. Supercooled Liquid Dynamics: Advances and Challenges. In *Structural Glasses and Supercooled Liquids: Theory, Experiment, and Applications*, Wolynes, P., Lubchenko, V., Eds. John Wiley & Sons, Inc.: Hoboken, NJ, 2012.
- (5) Ediger, M. D.; Forrest, J. A. Dynamics near Free Surfaces and the Glass Transition in Thin Polymer Films: A View to the Future. *Macromolecules* **2014**, *47*, 471–478.
- (6) Richert, R. Dynamics of Nanoconfined Supercooled Liquids. *Annu. Rev. Phys. Chem.* **2011**, *62*, 65–84.
- (7) Cangialosi, D. Dynamics and Thermodynamics of Polymer Glasses. *J. Phys.: Condens. Matter* **2014**, *26*, 153101.
- (8) Kaufman, L. J. Heterogeneity in Single-Molecule Observables in the Study of Supercooled Liquids. *Annu. Rev. Phys. Chem.* **2013**, *64*, 177–200.
- (9) Paeng, K.; Kaufman, L. J. Single Molecule Rotational Probing of Supercooled Liquids. *Chem. Soc. Rev.* **2014**, *43*, 977–989.
- (10) Flier, B. M. I.; Baier, M.; Huber, J.; Mullen, K.; Mecking, S.; Zumbusch, A.; Woll, D. Single Molecule Fluorescence Microscopy Investigations on Heterogeneity of Translational Diffusion in Thin Polymer Films. *Phys. Chem. Chem. Phys.* **2011**, *13*, 1770–1775.
- (11) Flier, B. M. I.; Baier, M. C.; Huber, J.; Mullen, K.; Mecking, S.; Zumbusch, A.; Woll, D. Heterogeneous Diffusion in Thin Polymer Films as Observed by High-Temperature Single-Molecule Fluorescence Microscopy. *J. Am. Chem. Soc.* **2012**, *134*, 480–488.
- (12) Habuchi, S.; Fujiwara, S.; Yamamoto, T.; Vacha, M.; Tezuka, Y. Single-Molecule Study on Polymer Diffusion in a Melt State: Effect of Chain Topology. *Anal. Chem.* **2013**, *85*, 7369–7376.
- (13) Paeng, K.; Lee, H. N.; Swallen, S. F.; Ediger, M. D. Temperature-Ramping Measurement of Dye Reorientation to Probe Molecular Motion in Polymer Glasses. *J. Chem. Phys.* **2011**, *134*, 024901.
- (14) Paeng, K.; Park, H.; Hoang, D. T.; Kaufman, L. J. Ideal Probe Single-Molecule Experiments Reveal the Intrinsic Dynamic Heterogeneity of a Supercooled Liquid. *Proc. Natl. Acad. Sci. U. S. A.* **2015**, *112*, 4952–4957.
- (15) Richert, R. On the Dielectric Susceptibility Spectra of Supercooled O-Terphenyl. *J. Chem. Phys.* **2005**, *123*, 154502.
- (16) Hoang, D. T.; Paeng, K.; Park, H.; Leone, L. M.; Kaufman, L. J. Extraction of Rotational Correlation Times from Noisy Single Molecule Fluorescence Trajectories. *Anal. Chem.* **2014**, *86*, 9322–9329.
- (17) Vallee, R. A. L.; Rohand, T.; Boens, N.; Dehaen, W.; Hinze, G.; Basche, T. Analysis of the Exponential Character of Single Molecule Rotational Correlation Functions for Large and Small Fluorescence Collection Angles. *J. Chem. Phys.* **2008**, *128*, 154515.
- (18) Mackowiak, S. A.; Herman, T. K.; Kaufman, L. J. Spatial and Temporal Heterogeneity in Supercooled Glycerol: Evidence from Wide Field Single Molecule Imaging. *J. Chem. Phys.* **2009**, *131*, 244513.
- (19) Paeng, K.; Swallen, S. F.; Ediger, M. D. Direct Measurement of Molecular Motion in Freestanding Polystyrene Thin Films. *J. Am. Chem. Soc.* **2011**, *133*, 8444–8447.
- (20) Paeng, K.; Richert, R.; Ediger, M. D. Molecular Mobility in Supported Thin Films of Polystyrene, Poly(Methyl Methacrylate), and Poly(2-Vinyl Pyridine) Probed by Dye Reorientation. *Soft Matter* **2012**, *8*, 819–826.

- (21) Plazek, D. J. Temperature Dependence of Viscoelastic Behavior of Polystyrene. *J. Phys. Chem.* **1965**, *69*, 3480–3487.
- (22) Roland, C. M.; Casalini, R. Temperature Dependence of Local Segmental Motion in Polystyrene and Its Variation with Molecular Weight. *J. Chem. Phys.* **2003**, *119*, 1838–1842.
- (23) Svanberg, C. Glass Transition Relaxations in Thin Suspended Polymer Films. *Macromolecules* **2007**, *40*, 312–315.
- (24) Lu, C. Y.; Vanden Bout, D. A. Effect of Finite Trajectory Length on the Correlation Function Analysis of Single Molecule Data. *J. Chem. Phys.* **2006**, *125*, 124701.
- (25) Mackowiak, S. A.; Kaufman, L. J. When the Heterogeneous Appears Homogeneous: Discrepant Measures of Heterogeneity in Single-Molecule Observables. *J. Phys. Chem. Lett.* **2011**, *2*, 438–442.
- (26) Stokely, K.; Manz, A. S.; Kaufman, L. J. Revealing and Resolving Degeneracies in Stretching Exponents in Temporally Heterogeneous Environments. *J. Chem. Phys.* **2015**, *142*, 114504.
- (27) Verma, S. D.; Vanden Bout, D. A.; Berg, M. A. When Is a Single Molecule Heterogeneous? A Multidimensional Answer and Its Application to Dynamics near the Glass Transition. *J. Chem. Phys.* **2015**, *143*, 024110.
- (28) Mackowiak, S. A.; Leone, L. M.; Kaufman, L. J. Probe Dependence of Spatially Heterogeneous Dynamics in Supercooled Glycerol as Revealed by Single Molecule Microscopy. *Phys. Chem. Chem. Phys.* **2011**, *13*, 1786–1799.
- (29) Robertson, C. G.; Santangelo, P. G.; Roland, C. M. Comparison of Glass Formation Kinetics and Segmental Relaxation in Polymers. *J. Non-Cryst. Solids* **2000**, *275*, 153–159.
- (30) Thureau, C. T.; Ediger, M. D. Influence of Spatially Heterogeneous Dynamics on Physical Aging of Polystyrene. *J. Chem. Phys.* **2002**, *116*, 9089–9099.
- (31) Wang, C. Y.; Ediger, M. D. Lifetime of Spatially Heterogeneous Dynamic Domains in Polystyrene Melts. *J. Chem. Phys.* **2000**, *112*, 6933–6937.
- (32) Leone, L. M.; Kaufman, L. J. Single Molecule Probe Reports of Dynamic Heterogeneity in Supercooled Ortho-Terphenyl. *J. Chem. Phys.* **2013**, *138*, 12a524.
- (33) Cicerone, M. T.; Blackburn, F. R.; Ediger, M. D. How Do Molecules Move near T-G - Molecular Rotation of 6 Probes in O-Terphenyl across 14 Decades in Time. *J. Chem. Phys.* **1995**, *102*, 471–479.
- (34) Wang, L. M.; Richert, R. Exponential Probe Rotation in Glass-Forming Liquids. *J. Chem. Phys.* **2004**, *120*, 11082–11089.
- (35) Ngai, K. L. Dynamic and Thermodynamic Properties of Glass-Forming Substances. *J. Non-Cryst. Solids* **2000**, *275*, 7–51.
- (36) Wang, C. Y.; Ediger, M. D. How Long Do Regions of Different Dynamics Persist in Supercooled O-Terphenyl? *J. Phys. Chem. B* **1999**, *103*, 4177–4184.